# Multistage Filtering Algorithm for Salt and Pepper Noise Removal from Highly Corrupted Microscopic Blood Images

Adem Alpaslan Altun
Information Technology Faculty
Selcuk University
Konya, Turkey
adem.altun@gmail.com

Hala Mulki
Computer Engineering Faculty
Selcuk University
Konya, Turkey
hallamulki@gmail.com

***Abstract*—Image quality mainly affects the performance of any medical image processing system. Salt & pepper noise is one type of noise that significantly degrades the image quality. Such noise can be frequently encountered in digital microscopic images due to technical reasons. Moreover, high ratios of Salt & pepper noise make the image excessively corrupted or unreadable. Standard and modified median filters can usually handle low/medium Salt & Pepper noise densities, mostly at the expense of edge/details preservation. However, they totally fail for highly corrupted images where noise density reaches 90%. In this paper, we present a new multistage filtering algorithm for Salt & pepper noise reduction from highly corrupted images while preserving image details and edges as better as possible. The proposed algorithm includes two filtering stages through which image is firstly de-noised via utilizing adaptive median filter then decision based median filter. Our multistage filter has been successfully applied on noisy microscopic blood images obtained from Malaria-infected blood smears. Results reveal that the presented filtering algorithm outperforms standard and modified median algorithms in terms of PSNR, MSE and IEF values, specifically for images with more than 80% of salt & pepper noise. This indicates that using our multistage filtering algorithm against high Salt & Pepper noise densities, does not only remove the noise effectively but also achieves a better edge and details preservation, hence a better image enhancement.**

***Index Terms*: salt & pepper noise, high noise density, spatial filtering algorithms, Standard Median Filters, Adaptive Median Filter, Decision Based Median Filter, Multistage Filter.**

## I. INTRODUCTION

Medical diagnosis is one of the most important fields in which digital image processing can be effectively applied. The correct diagnosis depends on the quality of the image from which the features will be extracted; hence, any degrade in the image quality may lead to a misdiagnosis [1]. Noise is the main reason of image corruption [1]; it usually arises at the image acquisition phase due to various factors. As for digital microscopic images, when transmission electron microscope or light microscope approach the resolution limit, noise appears as a random variation of brightness or color information causing a notable degrade in image quality [1].

Salt & pepper noise is one common type of impulse noise encountered in microscopic images in the form of randomly spread black and white dots, with which it is difficult to identify the real image components or to isolate infected objects [1]. Several filtering techniques have been utilized to reduce salt & pepper noise; most of them adopted spatial filtering methods, either linear or nonlinear filters. For low density of salt & pepper noise, linear Mean Filter (Average Filter) or AVGF is applied efficiently, it uses a window of a certain size that slides over the image, so that image smoothing is performed by replacing the center pixel value of the window with the average of all the neighboring pixel values including itself [1]. However, linear filters do not perform well when salt & pepper noise density increases, especially if we take into account the nonlinear nature of this noise [2].

To address this limitation, nonlinear filters have been proposed, represented by Standard Median Filter (SMF) and its variants. SMF also uses a sliding window within which all pixels are replaced by their median value, regardless the pixels' status (noisy or noise-free). Hence, the image fine details and edges may be lost [2]. In addition to that, the performance of SMF degrades for high noise densities, where it suffers from blurring for large window sizes and from insufficient noise reduction for small ones [3].

In order to achieve a better corners and edges preservation, Hybrid Median Filter (HMF) was presented in [4]. Here, the filtered value of a pixel in the current window is obtained via calculation of the median of three values which are: the horizontal and vertical pixels' median, diagonal pixels' median; and the value of the central pixel of the sliding window [4]. HMF offers a solution for edge treatment problem, since it can extend the image symmetrically to fill the gap resulted from applying the window over edge pixels [4]. Unlike standard median filter, HMF does not excessively smooth image details, but a high computation cost and low performance are met when handling high densities of salt & pepper noise [4].

Later, the switching concept emerged to improve the capability of the above-mentioned nonlinear filters, by taking the pixel's status into consideration, where a noisy pixel detection is performed before altering the pixels' values via the filtering technique [3]. The noisy pixel detection is usually achieved by using a criterion based on similarity to or difference from the central pixel within neighborhood [3,5].

IRJECE

A popular type of these filters is introduced in [6] so called Adaptive Median Filter (AMF). In this filter, noisy pixels are firstly identified by comparing each pixel in the image with pixels existed in the same filtering window, so that if this pixel is different from them, it is tagged as a noisy pixel. After that, all noisy pixels are replaced by the median value of the pixels in the neighborhood that have already passed the noise detection test. What distinguishes this filter is the adjustable window size of the neighborhood, i.e. the sliding window size is increased repeatedly until a noise-free median pixel is found or reaches the maximum [6]. AMF performs well at low noise densities, but at high ratios of noise, the window size has to be increased more often which is considered costly [7]. Besides, edge loss and blurring can be often occurred as a result of replacing a far pixel of very different properties with a noisy one [7].

To overcome inconsistency issues caused by the pixel replacement method, adopted by AMF, Decision Based Median filter (DBMF) has been proposed in [8]. Here, noisy pixel is replaced by noise-free one selected from a close area. This is done by replacing a noisy pixel with the median value of its current window, but in case that median is also noisy, the last processed pixel is used to replace the current one [8]. One advantage of this approach is that it is guaranteed to replace a noisy pixel with a noise-free one, but, if noise density is high, as the algorithm comes into a dense area where noise-free pixels cannot be found, a noisy pixel is replaced with the last clean processed one which may has a less consistency with pixels of the current window; In this case, the error is propagated, i.e. the smoothness and fine details get lost, yet this filter has an acceptable de-noising performance and a stable runtime [9]. All the above mentioned filters fail to handle noise in highly corrupted images where noise levels may reach 90%.

To address that issue, we present in this paper, a new filtering technique that can remove high densities of salt & pepper noise from microscopic images. The proposed filter consists of two filtering stages, in the first one, AMF is used to perform a primitive noise reduction, then in the next stage, DBMF is utilized to improve the noise removal process, so that, from a highly corrupted blood image an enhanced quite noise-free version can be obtained. The proposed filter has been examined over "cameraman" image, and successfully applied for highly corrupted malaria-infected blood images. The comparative results indicate a notable improvement in image quality especially for high densities of noise.

This paper is organized as follows; Section II introduces the salt & pepper noise model. In section III, image noise reduction algorithms are briefly described; while in section IV, the proposed filter is explained in detail. Section V gives the experimental results and comparative analysis. Finally, section VI concludes this study.

## II. SALT AND PEPPER NOISE MODEL

Image noise is an undesired and unavoidable variation in pixel intensity values. It quite often occurs during an image acquisition or transmission [6]. One common type of image noise is Salt & Pepper noise; which is caused by several factors such as analog-to-digital converter errors or overheated faulty components or due to fast recording and transmission [6].

In microscopic images, salt & pepper noise is encountered as a result of microscope defects or due to environmental conditions, system noise, motion of the object or bit errors in transmission [10]. We can easily recognize this type of noise in images, because of its bi-polar nature, for corrupted pixels are either of full brightness or of full blackness [11], that's why it is also known as fixed-valued impulse noise. Mathematically speaking, when an 8-bit representation is used for a digital image, the typical digitized intensity value for pepper noise is minimal (0) and for salt noise is maximal (255) in the dynamic range from 0 to 255[11], as in figure (1)

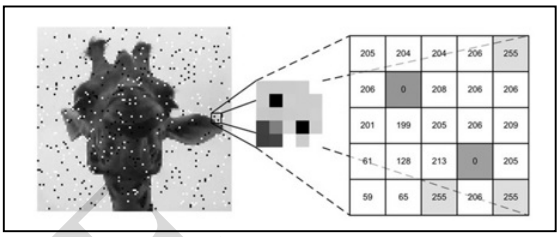


Fig. 1: Image corrupted with salt & pepper noise

The probability density function (PDF) of salt-and-pepper noise in a grayscale image can be expressed by Eq. 1:

$$PDF[g(x,y)] = \begin{cases} p/2 & \text{for } g(x,y) = 0 \\ 1-p & \text{for } g(x,y) = f(x,y) \\ p/2 & \text{for } g(x,y) = 255 \end{cases} \quad (1)$$

where p is the probability of degradation, g(x,y) is the intensity value of the corrupted image at (x,y), and f(x,y) is original intensity value.

## III. IMAGE DE-NOISING ALGORITHMS

Due to the variety of noise types, several filtering algorithms with different specifications have been introduced; they are classified into spatial domain filtering algorithms and frequency domain filtering algorithms [1].

### *A. Frequency Domain Filtering Algorithms*

Here, the image is Fourier transformed, multiplied with the filter function and then re-transformed into the spatial domain. Attenuating high frequencies results in a smoother image in the spatial domain, while attenuating low frequencies enhances the edges [12].

### *B. Spatial Domain Filtering Algorithms*

They involve a mask or window that slides all over the image; so that, to deduce the filtered value of a pixel, iteratively, a mathematical operation is performed on a set of pixels related to that pixel and existed in its neighborhood [12] as it is illustrated in figure (2)

IRJECE

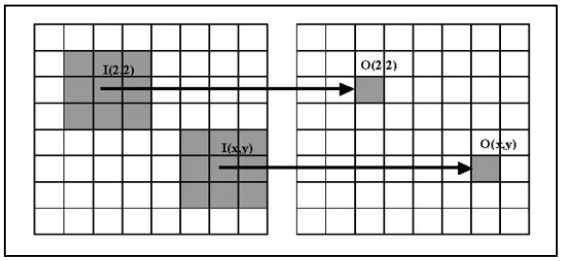


Fig. 2: Principle of the spatial domain filtering

Spatial domain filtering algorithms are the most basic and simple to use, and they are divided into linear and nonlinear filters.

- Linear Spatial filters: modify an image by replacing the value at each pixel with some linear function of the values of pixels from its neighborhood. Where this function is basically determined by the value of the window (mask) coefficients. One popular type of these filters is AVGF [13].
- Nonlinear Spatial Filters: do not follow the properties of additivity and homogeneity. They perform a nonlinear operation on the image pixels. For example, the Max filter finds the maximum value of the pixels in an image [14]. The simplest nonlinear filter to mention is the SMF.

Both linear and nonlinear spatial filters have their place in image processing functions; they are often related to the specifications of the targeted noise [14]. However, generally, linear spatial filters are usually fast enough, but tend to lose the details of the images [1], whereas nonlinear filters are more powerful especially for salt & pepper noise for they can achieve noise removal while preserving edges and details, such as median filter [14].

## IV. THE PROPOSED MULTISTAGE FILTERING ALGORITHM

With the availability of dozens of linear and nonlinear filters, it is not easy to decide which type of filter to select. However, the nature of the image data, the noise type and density, and a comparative performance analysis of several filters against this very noise, along with the ability of filters to be customized, may lead you to the convenient choice [14].

Regarding our case study, in which high density of salt & pepper noise should be removed from microscopic blood images, and considering the performance of previous filters examined in related research, we found that among the above mentioned filters in section I, in the case of high noise density, AMF can achieve a very good edge preservation, yet its performance for noise reduction is fair, due to the pixel replacement rule by which a median which represents a pixel from a far area may replace a noisy one[12]. On the other hand, DBMF with its robust replacement rule, is able to reasonably reduce high ratios of Salt & Pepper noise, but at the expense of fine details preservation [9]. So, in order to achieve a better noise reduction accompanied with an improved edge and fine details preservation, we combined the two filters AMF and DBMF as a multistage filtering algorithm as illustrated in figure (3), where AMF is referred to as 1 and DBMF as 2 in which the first stage is responsible for a primitive noise reduction carried out by AMF, whereas in the next stage, the resulted semi enhanced image forms the input of the DBMF, which in turn improves the low correlation between pixels, by using the replacement rule of DBMF while re-de-noising the image, so that the final resulted image is enhanced as best as possible.

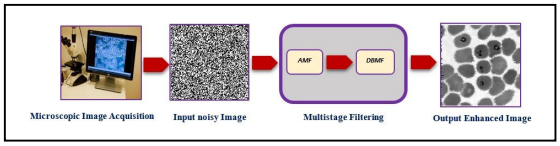


Fig. 3: The proposed multistage filter flowchart

### *A. Adaptive Median Filtering stage*

In the proposed filter, it is firstly used because of its ability of a moderate noise reduction along with a good edges preservation [15]. Unlike standard median filter, the filtering window size in AMF is not fixed; Its size varies due to the status of the pixel representing the median of the pixels included in the current window. Where, if the median pixel value is found noisy, then the window size is expanded. Otherwise, further processing is performed over the part of the image surrounded by the current window [12]. Before explaining the AMF algorithm step by step, let's denote the algorithm parameters as follows:

$S_{xy}$: the filtering window size or the neighborhood size, Zmin: minimum gray level value in $S_{xy}$, Zmax: maximum gray level value in Sxy, Zmed: median of gray levels in Sxy, Zxy: gray level at coordinates (x, y), Smax: maximum allowed size of $S_{xy}$, where the coordinates (x,y) indicate the pixel on which the current window is centered. The algorithm operates through two levels called level A and level B; they are clarified as follows:

- Level A: A1 = Zmed - Zmin
  A2 = Zmed - Zmax
  If A1 > 0 AND A2 < 0 (Zmed is not noisy),
- Go to Level B to check if Zxy is noisy else increase the window size (Zmed is noisy)
- if window size < Smax, repeats level A until Zmed if not noisy or Smax is reached else output Zxy
- Level B: B1 = Zxy – Zmin , B2 = Zxy – Zmax
- If B1 > 0 & B2 < 0 (Zxy is noise-free), output Zxy
- Else (Zxy is noisy) ➔ output Zmed

It has been observed that AMF performs well against low noise densities where a few noisy pixels have to be replaced by the median values. However, for highly corrupted images, window size is required to be increased, trying to find a noise-free median, regardless how far it is from the manipulated noisy pixel, this causes inconsistency between noisy pixels and replaced median pixels hence affects the image enhancement degree [6].

IRJECE

*B. Decision based median filtering stage*

In this stage, a decision based median filter DBMF is used to enhance the image resulted from the previous stage. DBMF algorithm uses a fixed filtering window size of 3x3; for each pixel in the current filtering window, a test is firstly performed to discover noisy pixels by checking whether a pixel's value equals to the minimum value (0) or the maximum value (255), since salt & pepper noise of bipolar nature such as that takes the values 0 or 255. Later, a robust pixel replacement rule is applied in which noisy pixels are replaced by either the median pixel or a pixel from its close neighborhood [16]. The algorithm manipulates each pixel in the current window as follows:

- Step 1. if this pixel's value equals 0 or 255, then it is a noisy pixel, else (noise-free) go to step 5
- Step 2. if the median pixel value lies between 0 and 255 then it is noise-free, else go to step 4
- Step 3. Replace the noisy pixel with the median value of the neighborhood surrounded by the current window then go to step 5.
- Step 4. In case of noisy median, replace the noisy pixel by the previously processed left neighborhood pixel's value.
- Step 5. Take the next pixel.

These steps are repeated until all the pixels are processed. Using DBMF as a second filtering stage provides a good solution to address the lack of correlation among image pixels that occurred in the first filtering stage; hence, an improved noise reduction and edge preservation are achieved.

## V. SIMULATED RESULTS AND ANALYSIS

The proposed multistage filter, has been tested over 8-bit grayscale images of size 512 X 512 and 7X7 window, corrupted by salt & pepper noise with different density levels ranges from 10% up to 90%. Results of the proposed filter were compared with SMF, Average Filter, HMF, AMF, DBMF filters, using several important measurement parameters, such as the peak signal to noise ratio (PSNR) which is a good indicator of the noise reduction quality [2].

Since if PSNR is large, it means that the content of signal in the output is large and the noise is less [17]. PSNR is calculated via Eq.2.

$$PSNR=10\log_{10}(255\text{^}2/MSE) \qquad (2)$$

Where MSE is the second measurement parameter stands for the Mean Square Error, and is given by Eq. 3.

$$MSE = \frac{1}{MN}\sum_{j-1}^{M}\sum_{k-1}^{N}(xj,k - x'j,k) \qquad (3)$$

Where, *M* and *N* are image rows and columns respectively, *xj,k* is the input image and $x'_{j,k}$ is the output image. MSE refers to the difference in the pixel intensity of the input and output image [2]. So, when it is less, this indicates a good noise reduction, since pixel intensity of the input and filtered image are then close to each other [17].

Thus, the greater the PSNR value is, the less the MSE value is, the better the de-noising performance becomes [2].

The last measurement parameter that also evaluates the de-noising performance of the used filter [2,17], is the Image Enhancement Factor (IEF); it is expressed by Eq. 4.

$$IEF = \frac{\sum_{i=1}^{m}\sum_{j=1}^{n}(yi,j - xi,j)^2}{\sum_{i=1}^{m}\sum_{j=1}^{n}(zi,j - xi,j)^2} \qquad (4)$$

Where, $x_{i,j}$: the original input image, $y_{i,j}$: the noisy image, $z_{i,j}$: the de-noised output image, *m* and *n* are image rows and columns respectively. Experimental results have been carried out first using standard test images like "cameraman" and "Baboon", then by using case study microscopic images obtained from the Centers for Disease Control & prevention (CDC) website [18].

Figure (4) and figure (5), represent comparative results of applying previous filters over cameraman and baboon respectively, where the presented filter is denoted as PA.

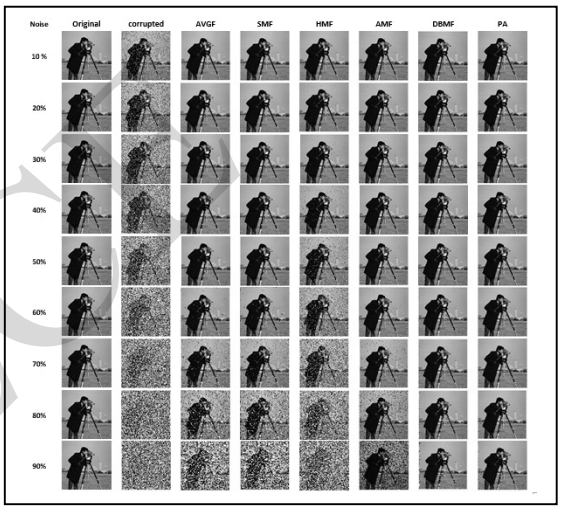


Fig. 4: De-noised Cameraman image using different filters

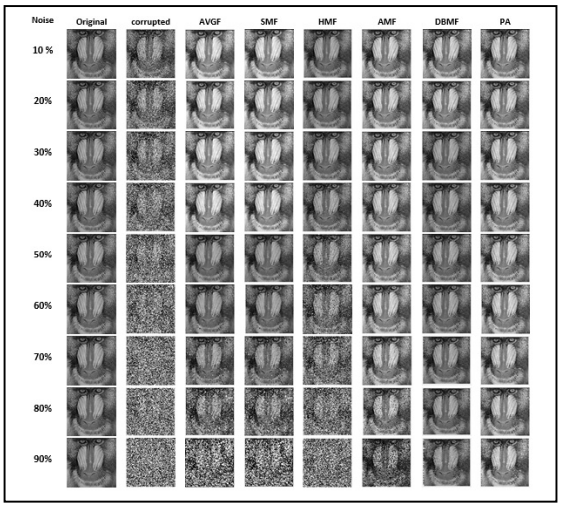


Fig. 5: De-noised Baboon image using different filters

Table (I) and table (II) include PSNR, MSE and IEF values of all the filters and different noise densities for

IRJECE

cameraman image, while table (III) and table (IV) report the same parameters for the baboon image.

Table I: PSNR, MSE values of the Cameraman image

| Noise Density | PSNR | | | | | | MSE | | | | | |
|---|---|---|---|---|---|---|---|---|---|---|---|---|
| | *AVGF* | *SMF* | *HMF* | *AMF* | *DBMF* | *PA* | *AVGF* | *SMF* | *HMF* | *AMF* | *DBMF* | *PA* |
| 10 % | 23.35 | 27.15 | 32.42 | 39.48 | 41.29 | 40.11 | 300.47 | 125.24 | 37.21 | 7.32 | 4.82 | 6.33 |
| 20% | 21.38 | 25.49 | 29.73 | 36.37 | 36.91 | 36.40 | 472.33 | 183.52 | 69.10 | 14.97 | 13.23 | 14.87 |
| 30% | 19.70 | 24.37 | 26.40 | 33.82 | 33.89 | 33.83 | 696.04 | 237.63 | 148.75 | 26.97 | 26.51 | 26.90 |
| 40% | 18.06 | 23.29 | 21.28 | 31.56 | 31.42 | 31.58 | 1015.77 | 304.44 | 483.27 | 45.30 | 46.79 | 45.13 |
| 50% | 16.74 | 22.29 | 17.09 | 29.53 | 29.28 | 29.64 | 1375.02 | 383.38 | 1270.26 | 72.42 | 76.62 | 70.56 |
| 60% | 15.50 | 20.66 | 13.36 | 26.81 | 26.99 | 27.91 | 1830.05 | 557.69 | 2997.69 | 135.27 | 130 | 105.04 |
| 70% | 14.51 | 17.35 | 10.57 | 21.71 | 24.93 | 26.02 | 2299.30 | 1195.26 | 5697.74 | 437.93 | 208.94 | 162.37 |
| 80% | 13.45 | 12.38 | 8.22 | 15.84 | 22.38 | 23.91 | 2934.33 | 3750.44 | 9796.02 | 1694.02 | 375.89 | 263.71 |
| 90% | 12.62 | 8.13 | 6.47 | 10.40 | 18.85 | 21.45 | 3548.88 | 9989.93 | 14639.01 | 5929.10 | 846.01 | 464.93 |

Table II: IEF values of the Cameraman image

| Noise Density | IEF | | | | | |
|---|---|---|---|---|---|---|
| | *AVGF* | *SMF* | *HMF* | *AMF* | *DBMF* | *PA* |
| 10 % | 6.71 | 16.10 | 54.20 | 275.56 | 417.73 | 318.63 |
| 20% | 8.61 | 22.17 | 58.88 | 271.76 | 307.52 | 273.48 |
| 30% | 8.67 | 25.42 | 40.61 | 223.94 | 227.86 | 224.56 |
| 40% | 7.96 | 26.57 | 16.74 | 178.61 | 172.92 | 179.26 |
| 50% | 7.32 | 26.26 | 7.92 | 139.01 | 131.39 | 142.66 |
| 60% | 6.62 | 21.72 | 4.04 | 89.58 | 93.21 | 115.36 |
| 70% | 6.11 | 11.75 | 2.46 | 32.08 | 67.25 | 86.54 |
| 80% | 5.50 | 4.30 | 1.64 | 9.54 | 42.99 | 61.28 |
| 90% | 5.10 | 1.81 | 1.23 | 3.05 | 21.42 | 38.97 |

Table III: PSNR, MSE values of the Baboon image

| Noise density | PSNR | | | | | | MSE | | | | | |
|---|---|---|---|---|---|---|---|---|---|---|---|---|
| | *AVGF* | *SMF* | *HMF* | *AMF* | *DBMF* | *PA* | *AVGF* | *SMF* | *HMF* | *AMF* | *DBMF* | *PA* |
| 10 % | 23.87 | 25.84 | 30.19 | 39.07 | 40.71 | 39.04 | 266.40 | 169.14 | 62.15 | 8.05 | 5.51 | 8.10 |
| 20% | 22.44 | 25.35 | 28.92 | 35.86 | 36.48 | 35.86 | 370.07 | 189.63 | 83.19 | 16.83 | 14.61 | 16.86 |
| 30% | 21 | 24.61 | 25.80 | 33.35 | 33.37 | 33.34 | 516.32 | 224.47 | 170.82 | 30.02 | 29.88 | 30.07 |
| 40% | 19.69 | 24.15 | 21.60 | 31.19 | 31.16 | 31.20 | 698.02 | 249.73 | 449.84 | 49.34 | 49.68 | 49.32 |
| 50% | 18.53 | 23.45 | 17.30 | 29.31 | 29.24 | 29.35 | 911.64 | 293.65 | 1210.24 | 76.08 | 77.45 | 75.50 |
| 60% | 17.39 | 22.16 | 13.76 | 27.09 | 27.24 | 27.66 | 1184.95 | 395.26 | 2733.39 | 126.82 | 122.61 | 111.38 |
| 70% | 16.36 | 18.12 | 10.84 | 23.09 | 25.46 | 25.90 | 1502.24 | 1002.24 | 5358.63 | 319.15 | 184.73 | 166.94 |
| 80% | 15.52 | 13.03 | 8.60 | 17.51 | 23.30 | 24.05 | 1820.27 | 3235.17 | 8971.85 | 1151.45 | 304.08 | 255.60 |
| 90% | 14.63 | 8.46 | 6.76 | 12.24 | 19.95 | 21.76 | 2237.78 | 9256.61 | 13692.61 | 3877.70 | 657.01 | 432.84 |

Table IV: IEF values of the Baboon image

| Noise density | IEF | | | | | |
|---|---|---|---|---|---|---|
| | *AVGF* | *SMF* | *HMF* | *AMF* | *DBMF* | *PA* |
| 10 % | 6.99 | 11.01 | 29.98 | 231.43 | 337.93 | 229.84 |
| 20% | 10.01 | 19.55 | 44.57 | 220.28 | 253.64 | 219.84 |
| 30% | 10.80 | 24.85 | 32.65 | 185.77 | 186.65 | 185.46 |
| 40% | 10.62 | 29.69 | 16.48 | 150.31 | 149.27 | 150.38 |
| 50% | 10.19 | 31.63 | 7.67 | 122.09 | 119.94 | 123.04 |
| 60% | 9.42 | 28.25 | 4.08 | 88.05 | 91.08 | 100.26 |
| 70% | 8.67 | 13 | 2.43 | 40.84 | 70.56 | 78.08 |
| 80% | 8.16 | 4.59 | 1.65 | 12.90 | 48.86 | 58.13 |
| 90% | 7.49 | 1.81 | 1.22 | 4.32 | 25.53 | 38.75 |

We can notice from table I and table II, that when noise density is below 50%, AMF, DBMF and PA have a close performance in terms of PSNR and MSE values, since at these densities AMF does not have to extend the filtering window so frequent; hence, pixels' replacement procedure tends to be carried out in the same window, so adding DBMF as a next filtering stage will not improve the performance so much. However, for noise densities above 50 %, most of the filters' performance become weak, especially the HMF.

However, for very high noise densities such as 80% and 90%, the outperformance of the proposed filter is clearly noted. For, as noise density increases, AMF keeps extending the filtering window trying to find a noisy-free median to replace current window's noisy pixels, regardless how far is this median from the current area, which results in less correlation ratio between pixels [6].

Figure (6) show the comparative results of applying previous filters over blood images of malaria-infected smears, where the presented filter is denoted as PA. While table V and table VI include PSNR, MSE and IEF values.

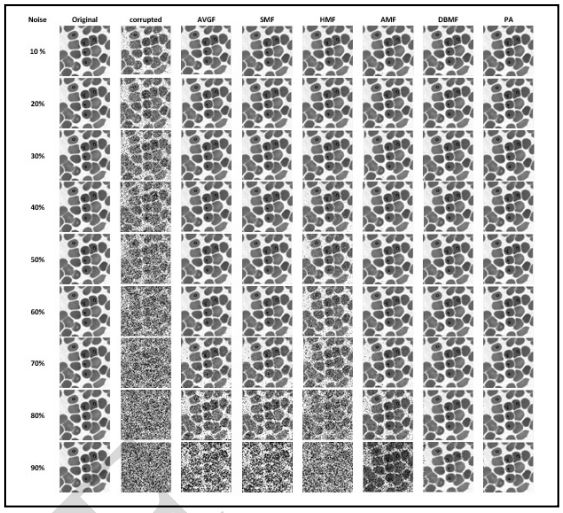


Fig. 6: Filtered output of the microscopic blood image

Table (V) and table (VI) include PSNR, MSE and IEF values of all the filters and different noise densities for the blood image.

Table V: PSNR, MSE values of the microscopic blood image

| Noise density | PSNR | | | | | | MSE | | | | | |
|---|---|---|---|---|---|---|---|---|---|---|---|---|
| | *AVGF* | *SMF* | *HMF* | *AMF* | *DBMF* | *PA* | *AVGF* | *SMF* | *HMF* | *AMF* | *DBMF* | *PA* |
| 10 % | 25.55 | 36.04 | 41.75 | 38.84 | 48.92 | 48.17 | 181.15 | 16.17 | 4.34 | 8.84 | 0.83 | 0.98 |
| 20% | 22.41 | 28.87 | 36.03 | 38.85 | 43.72 | 43.70 | 372.59 | 84.19 | 16.22 | 8.46 | 2.75 | 2.76 |
| 30% | 19.96 | 26.35 | 29.07 | 37.82 | 40.03 | 40.70 | 655.60 | 150.44 | 80.42 | 10.71 | 6.45 | 5.52 |
| 40% | 18.10 | 24.72 | 22.26 | 35.71 | 37.36 | 38.22 | 1006.72 | 219.06 | 385.64 | 17.43 | 11.93 | 9.78 |
| 50% | 16.51 | 23.39 | 17.47 | 34.17 | 35.29 | 35.99 | 1449.46 | 297.62 | 1161.81 | 24.84 | 19.22 | 16.36 |
| 60% | 15.18 | 21.40 | 13.56 | 29.43 | 32.38 | 33.92 | 1971.81 | 470.65 | 2860.98 | 74.02 | 37.56 | 26.34 |
| 70% | 13.95 | 17.75 | 10.49 | 21.63 | 29.32 | 31.50 | 2612.84 | 1090.03 | 5808.36 | 446.22 | 75.90 | 45.94 |
| 80% | 12.85 | 12.26 | 8.10 | 14.43 | 25.41 | 28.49 | 3366.50 | 3858.85 | 10070.66 | 2344.11 | 186.78 | 92.04 |
| 90% | 12.02 | 8.05 | 6.34 | 8.86 | 20.73 | 24.62 | 4082.98 | 10166.81 | 15098.22 | 8448.23 | 548.98 | 224.24 |

Table VI: IEF values of the microscopic blood image

| Noise density | IEF | | | | | |
|---|---|---|---|---|---|---|
| | *AVGF* | *SMF* | *HMF* | *AMF* | *DBMF* | *PA* |
| 10 % | 11.43 | 128.03 | 476.87 | 244.10 | 2485.18 | 2094.36 |
| 20% | 11.11 | 49.19 | 255.32 | 489.52 | 1502.43 | 1495.75 |
| 30% | 9.55 | 41.64 | 77.89 | 584.43 | 971.09 | 1134.50 |
| 40% | 8.25 | 37.95 | 21.55 | 476.90 | 696.79 | 849.82 |
| 50% | 7.16 | 34.87 | 8.93 | 417.78 | 540 | 634.22 |
| 60% | 6.30 | 26.42 | 4.34 | 168.02 | 331.07 | 472.13 |
| 70% | 5.57 | 13.37 | 2.50 | 32.66 | 192.02 | 317.21 |
| 80% | 4.96 | 4.32 | 1.65 | 7.12 | 89.42 | 181.47 |
| 90% | 4.58 | 1.84 | 1.23 | 2.21 | 34.09 | 83.47 |

The previous tables (V, VI) show that using our filter decrease the MSE to the half at 90% noise density, and achieves the highest value of PSNR and IEF parameters, which proves the outperformance of the multistage filter over the other filters, particularly at high noise densities, where it can restore a quite clear image from a highly corrupted one as in figure (6). Results of the evaluation parameters PSNR,

REJECT

MSE and against different noise densities for all studied filters can also be presented by the charts in figures (7), (8), (9) respectively.

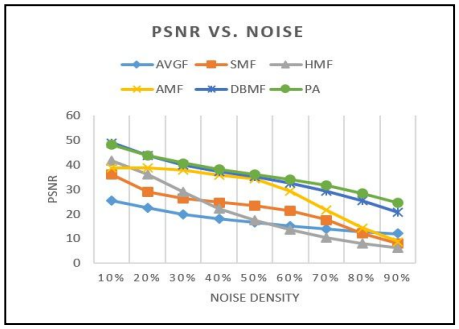


Fig. 7: PSNR VS. noise for all filters used on the blood image

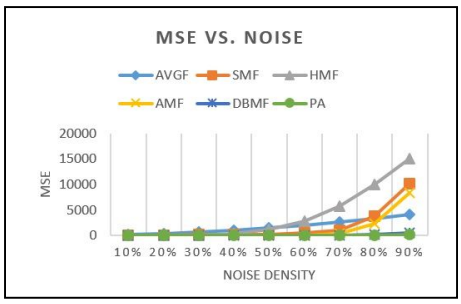


Fig. 8: PSNR VS. noise for all filters used on the blood image

## VI. CONCLUSION

In this paper, a new multistage filtering algorithm has been proposed to remove Salt & Pepper noise from highly corrupted microscopic blood images. The new filter was designed according to the performance analysis of several filters against high density levels of salt & pepper noise. It has been noted that AMF and DBMF were better than other median filter variants. So that, they both selected to form the components of the proposed filter. A better enhancement of a highly corrupted images was achieved using this filter, where two filtering stages exist, in the first one primitive noise reduction and edge preservation is performed by AMF, whereas the second stage receives the image resulted from the previous stage as an input, then re-reduce noise from it using DBMF. Due to the robust pixel replacement rule adopted by DBMF, an improvement in the correlation ratio between the pixels of the final output image has been observed. This result was verified through simulation experiments, where the proposed filter was examined and compared with various filters, for de-noising standard test images and microscopic blood images corrupted by high density of salt & pepper noise. Experiments show that, the proposed multistage filter outperformed the other filters in terms of PSNR and MSE values, which makes it an effective filtering tool to be used against high density levels of salt & pepper noise.

## REFERENCES

[1] S. Dangeti, "Denoising Techniques - A Comparison," M.S. thesis, Dept. Electrical. Computer. Eng., Louisiana State Univ., USA, 2003.

[2] A. Majid and M. T. Mahmood, "A novel technique for removal of high density impulse noise from digital images," Proc. - 2010 6th Int. Conf. Emerg. Technol. ICET 2010, pp. 139–143,2010.

[3] U. Ghanekar, A. K. Singh, and R. Pandey, "A contrast enhancement-based filter for removal of random valued impulse noise," IEEE Signal Process. Lett., vol. 17, no. 1, pp. 47–50, 2010.

[4] M. R. Rakesh, B. Ajeya, and a R. Mohan, "Hybrid Median Filter for Impulse Noise Removal of an Image in Image Restoration," pp. 5117–5124, 2013.

[5] Z. Xu, H. R. Wu, B. Qiu, and X. Yu, "Geometric features-based filtering for suppression of impulse noise in color images," IEEE Trans. Image Process., vol. 18, no. 8, pp. 1742–1759, 2009.

[6] H. Hwang and R. A. Haddad, "Adaptive Median Filters: New Algorithms and Results," IEEE Trans. Image Process., vol. 4, no. 4, pp. 499–502, 1995.

[7] H. Yu, L. Zhao, and H. Wang, "An efficient procedure for removing random-valued impulse noise in images," IEEE Signal Process. Lett., vol. 15, no. 2, pp. 922–925, 2008.

[8] K. S. Srinivasan and D. Ebenezer, "A new fast and efficient decision-based algorithm for removal of high-density impulse noises," IEEE Signal Process. Lett., vol. 14, no. 3, pp. 189–192, 2007.

[9] A. Jourabloo, A. H. Feghahati, and M. Jamzad, "New algorithms for recovering highly corrupted images with impulse noise," Sci. Iran., vol. 19, no. 6, pp. 1738–1745, 2012.

[10] N. G. Smrity Prasad, "An Efficient Approach for Image Filtering by Using Neighbors pixels," Int. J. Adv. Comput. Sci. Appl., vol. 4, no. 6, pp. 133–138, 2013.

[11] J. Xu and T. D. Pham, "Robust impulse-noise filtering for biomedical images using numerical interpolation," Lect. Notes Artif. Intell. Bioinformatics., vol. 7325 LNCS, no. PART 2, pp. 146–155, 2012.

[12] C. Science, S. Vincent, and P. College, "A Review of Decision Based Impulse Noise Removing Algorithms," vol. 4, no. 4, pp. 54–59, 2014.

[13] A. Azarimoghaddam and L. Rangarajan, "A Novel Algorithm for De-Noising Radiographic Images," Int. J. Image, Graph. Signal Process., vol. 4, no. 6, pp. 22–28, 2012.

[14] P. Garhwal and P. Garhwal, "Image Denoising with Linear and Non-Linear Filters: A," vol. 10, no. 6, pp. 149–154, 2013.

[15] P. Wei, J. Li, D. Lu, and G. Chen, "A Fast and reliable switching median filter for highly corrupted images by impulse noise," 2007 IEEE Int. Symp. Circuits Syst. ISCAS 2007, pp. 3427–3430, 2007.

[16] R. Ma and S. Cheng, "Transactions Letters," *October*, vol. 59, no. 10, pp. 2641–2647, 2011.

[17] I. Engineering, "Removal of High Density Salt & Pepper Noise Using Modified Decision Based Un-Symmetric Trimmed Median Filter," vol. 2, no. 2, pp. 761–763, 2013.

[18] http://www.cdc.gov/dpdx/malaria/gallery.html

IRJECE